IJE TRANSACTIONS A: Basics Vol. 26, No. 10, (October 2013) 1225-1234

International Journal of Engineering

Journal Homepage: www.ije.ir

Multi-objective Optimization of a Projectile Tip for Normal Penetration

A. Khalkhali[a]*, S. Roshanfekr[b]

[a] *School of Automotive Engineering, Iran University of Science and Technology, Tehran, Iran*
[b] *School of Mechanical Engineering, Islamic Azad University, Takestan branch, Qazvin, Iran*

PAPER INFO

Paper history:
Received 30 January 2013
Received in revised form 04 March 2013
Accepted 18 April 2013

Keywords:
Projectile
Impact
Finite Element Method
Neural Networks
Multi-objective Optimization
NSGA-II

ABSTRACT

The main purpose of the present work is multi-objective shape optimization of a projectile tip for impacting and normal penetrating. Velocity drop, weight and inner volume of projectile have been considered as three conflicting objective functions. For this purpose, at the first step, finite element modeling was done using ABAQUS/Explicit and projectile penetration was examined in different geometric dimensions. Hammersley sequence sampling was employed for designing computer experiments. In the next step, results of the FEM were employed as raw data for MLF-type neural network training to achieve a mathematical model which is able to describe velocity drop behavior. Projectile weight and Inner volume were also expressed in explicit mathematical form using geometric relations. Obtained mathematical models were used as conflicting objective functions for multi-objective optimization of projectile tip using modified NSGA-II. Finally, it is shown that some interesting and important relationships as useful optimal design principles involved in the performance of projectile impact have been discovered by Pareto based multi-objective optimization.

doi: *10.5829/idosi.ije.2013.26.10a.12*

1. INTRODUCTION

Researches on projectile penetration can be divided into two main classes. The first class is related to the performance of projectile penetration and the second one is about the performance of penetration resistance. Analytical and experimental studies on the ballistic resistance of thin, flat beams of pure aluminum and 6061-T6 aluminum alloy, was done by Marom and Bonder [1]. They showed that the multi-layered beams in contact have greater penetration resistance than monolithic beams under the same conditions. Corran et al. [2] carried out research on the performance of multilayered steel plates under projectile impact. They showed that the layers placed in contact were superior to equivalent monolithic plates when the response of individual plates changed from petalling and shearing to membrane stretching. Investigation of the penetration resistance of layered steel plates using conical and flat nosed projectiles was conducted by Nurick and Walter [3]. The ballistic limit of monolithic plates was 4-8% higher than that of the in-contact layered targets under the same conditions. Gupta and Madhu [4, 5] showed for relatively thicker plates in two layers, the residual velocity was comparable to single plate of equivalent thickness. Nevertheless, for thin plates, in-contact layered combination gave higher residual velocity for all the materials tested. Borvik et al. [6, 7] investigated the behavior of 12mm thick single steel plates impacted by blunt, conical and hemispherical nosed projectiles of 20mm diameter. They showed that experimental and corresponding finite element results are in good agreement. Blunt nosed projectiles were more efficient penetrators than hemispherical and conical projectiles at low velocities. At higher impact velocities however, conical nosed projectiles required least energy to perforate the target plates. In 2012, Nilakantan [8], as a new approach, considered the effects of projectile characteristics on the probabilistic impact response of single-layer fully-clamped flexible woven fabrics is numerically studied and the probabilistic fabric impact response is observed to be strongly dependent on the shape of the projectile's impact face and the manner of

* Corresponding Author Email: ab_khalkhali@iust.ac.ir (A. Khalkhali)

projectile–yarn interactions at the impact site. Zhang Wei et al. [9], as an engineering approach conducted an experimental investigation on the ballistic performance of monolithic and layered metal plates. In 2013, Iqbal et al. [10] studies the impact of double-nosed projectile on aluminum plates. They observed that 0.82 mm thick target offered highest ballistic limit for blunt–blunt projectile, and 1.82 mm thick target offered highest ballistic limit for single-nose blunt projectile.

Optimal design of projectiles is related to many competing criteria such as minimizing velocity drop, minimizing projectile weight and maximizing projectile inner volume. Therefore, to consider all such criteria simultaneously, a complex multi-objective optimization problem (MOP) must be solved. Many different methods have been proposed by previous researchers for solving MOPs [11-15]. Non-dominated Sorting Genetic Algorithm (NSGA-II) which is Pareto based approach and one of the efficient algorithms for solving MOPs was proposed by Deb et al. [11]. It generates a set of non-dominated solutions (Pareto solutions), where a non-dominated solution performs better on at least one criterion than the other solutions. To improve NSGA-II, Nariman-Zadeh proposed modified NSGA-II which use ε-elimination algorithm instead of crowding factor [12]. This method has been employed successfully in many recent studies [16, 17].

System identification techniques are applied in many fields in order to model and predict the behaviors of unknown and/or very complex systems based on given input–output data [18]. Theoretically, in order to model a system, it is required to understand the explicit mathematical input–output relationship precisely. Such explicit mathematical modeling is, however, very difficult and is not readily tractable in poorly understood systems. Alternatively, soft computing methods [19], which concern computation in an imprecise environment, have gained significant attention. The main components of soft computing, namely fuzzy logic, neural networks and evolutionary algorithms, have shown great ability in solving complex non-linear system identification and control problems.

In the present work, the optimal design of a projectile tip was performed considering three objective functions namely, projectile velocity drop, projectile weight and projectile inner volume. In the first instance, a finite element model using ABAQUS/Explicit was generated for modeling projectile penetration through target made of steel 1045. Hammersley Sequence Sampling was then exploited for design of experiments so that the whole search space could be covered uniformly. After evaluation of all designed experiments using finite element model, a data base of inputs-outputs was generated. A multi-layered feed-forward-type (MLF) neural network was applied as a common powerful system identifier for describing projectile velocity drop behavior. Finally, a multi-objective evolutionary based optimization using modified NSGA-II was performed for achieving Pareto-optimal set which constitute some important and informative design principles which can be used efficiently as optimal performance of projectile penetration.

2. HAMMERSLEY SEQUENCE SAMPLING

Thanks to steady and continuing growth of computational power, studying physical process and engineering problems through deterministic computer simulated experiments has become very popular. But, generally these experiments are computationally expensive. As an example, evaluation of a finite element model can take from a few minutes up to several hours. Therefore, notable attempts have been made to develop cheaper and accurate surrogate models as a replacement for optimization and reliability analysis tasks. In order to achieve an appropriate surrogate model, choosing an efficient method for sampling technique or Design of Experiments (DOE) can play a vital role.

Classical experimental methods are those applied for physical experiments so that the principle of randomization, replication and blocking are respected in this class of experimental methods. However, on contrast, the aforementioned considerations are irrelevant when it comes to *deterministic* computer experiments. Thus, space-filling designs have been suggested for computer simulated experiments [20] to treat all regions of the design space equally. Orthogonal arrays [21], Latin hypercube sampling (LHS) [22], Hammersley sequences [23] and uniform designs [24] are space-filling designs have attracted more attention than others in the literature. Hammersley sequence sampling (HSS), which uses an optimal design scheme for placing the n points on a k-dimensional hypercube, has been found to provide better uniformity and either faster than Latin hypercube designs for a multi-dimensional unit hypercube [23]. The HSS sampling technique will be used in the present work to design the experiments for finite element model analyzing.

The algorithm that generates a Hammersley sequence makes use of the radix-R (R is an integer) notation of an integer. Any integer P can be presented through radix-R as below:

$$P = p_m p_{m-1} \cdots p_2 p_1 p_0 \tag{1}$$

$$P = p_0 + p_1 R + p_2 R^2 + \cdots + p_m R^m \tag{2}$$

Where $m = [\log_R n]$ (square brackets denote the integer part) and p_m to p_0 are digits of integer P. By reversing the order of the digits of P around the decimal point, a unique number in the interval [0 1) can be generated.

This number is called *inverse radix number* and can be stated as follows:

$$\varphi_R = .p_0 p_1 p_2 \dots p_m \quad (3)$$

$$\varphi_R = p_0 R^{-1} + p_1 R^{-2} + \dots + p_m R^{-m-1} \quad (4)$$

Thus, a set of *N* Hammersley points on a *k*-dimensional hypercube is as follows:

$$\vec{z}_k(n) = \left(\frac{n}{N}, \varphi_{R_1}(n), \varphi_{R_2}(n), \dots, \varphi_{R_{k-1}}(n)\right); \quad n = 1,2,\dots,N \quad (5)$$

where R_1, R_2, …,R_{k-1} are first *k-1* prime numbers.

3. MODELING OF MATERIAL BEHAVIOR

As the deformation of both projectile and target occur at high strain rate, modeling of material behavior should be conducted according to this high strain rate. In this regard, different models have been developed to describe material behavior for high strain rates. Johnson-Cook model which expresses plastic and disruptive behavior of material, have attracted lots of attention to solve problems involving high strain rates. Three main parts of Johnson-Cook [25] modeling are stiffness strain effect, strain rate effect and effect of temperature. These three important factors can be incorporated in Equation (6) to describe material behavior.

$$\bar{\sigma} = [A + B(\bar{\varepsilon}^{pl})^n][1 + Cln(\frac{\dot{\bar{\varepsilon}}^{pl}}{\dot{\varepsilon}_0})](1 - (\frac{T-T_0}{T_{melt}-T_0})^m) \quad (6)$$

where A, B, C, n and m are constant values which can be calculated for different materials through some special tests. The parameter $\bar{\varepsilon}^{pl}$ is equivalent value for plastic strain, $\dot{\bar{\varepsilon}}^{pl}$ the value of equivalent strain rate, $\dot{\varepsilon}_0$ the symbol for describing reference strain rate, T current temperature, T_{melt} the melting point temperature, and T_0 the room temperature. In the present paper, S7 and 1045 Steel have been chosen as materials for the projectile and the target, respectively. The corresponding Johnson-Cook coefficients are given in the Table 1 [26].

In addition to modeling plastic behavior of material, another model known as Johnson-Cook fracture model has been presented. In this model, it is supposed that rupture phenomena occurs when value of a variable named D reaches 1.

TABLE 1. Coefficient of Johnson-Cook plastic behavior equation applied materials [26]

Material	A	B	n	C	m
S7	1539	447	0.18	0.012	1
St 1045	553	600	0.234	0.0134	1

The aforementioned variable which is called damage criterion mathematically can be stated as follows:

$$D = \sum(\frac{\Delta\bar{\varepsilon}^{pl}}{\bar{\varepsilon}_f^{pl}}) \quad (7)$$

where $\Delta\bar{\varepsilon}^{pl}$ denotes equivalent plastic strain rate and $\bar{\varepsilon}_f^{pl}$ denotes equivalent strain in fracture so that all the rates are accumulated. In Equation (7), $\bar{\varepsilon}_f^{pl}$ can be calculated in accordance with the equation given below:

$$\bar{\varepsilon}_f^{pl} = \left[D_1 + D_2 e^{\left(D_3\frac{\sigma_m}{\bar{\sigma}}\right)}\right]\left[1 + D_4 \ln\left(\frac{\dot{\bar{\varepsilon}}^{pl}}{\dot{\varepsilon}_0}\right)\right] + \left(1 + D_5\left(\frac{T-T_0}{T_{melt}-T_0}\right)\right) \quad (8)$$

where the coefficients D_1 to D_5 are constants, σ_m/σ_{eq} is the stress triaxiality ratio, and σ_m the mean stress; and other parameters have been defined earlier. ABAQUS/Explicit software is able to define plastic behavior of the material and also fracture behavior based on Johnson-Cook equations so that the software has the capability to delete elements with value of 1 for fracture criterion (*D*) using element deletion algorithms. Thus, fracture phenomena can be modelled. Table 2 provides values of coefficients of Johnson-Cook fracture equation for the target material (steel 1045).

4. FINITE ELEMENT ANALYSIS OF IMPACT AND NORMAL PENETRATION OF PROJECTILE

To analyze behavior of projectile penetration, a finite element model has been developed. Figure 1 represents projectile shape and geometrical variables. Radius of the tip (*r*), angle of the tip (θ) and wall thickness (*t*) of the projectile are considered as geometrical parameters which affect its penetration behavior.

TABLE 2. Coefficient of Johnson-Cook departure equation

Material	D_1	D_2	D_3	D_4	D_5
St 1045	553	600	0.234	0.0134	1

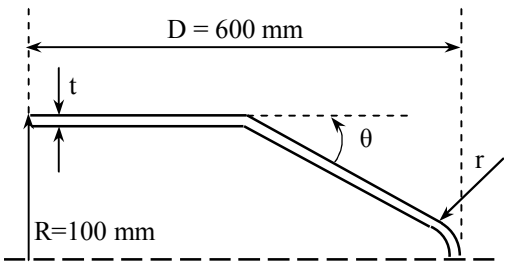

Figure 1. Geometrical variables and projectile shape

TABLE 3. Some of the geometrical variables and finite element results for normal penetration

No.	r (mm)	θ (deg)	t (mm)	Velocity Drop (m/s)
1	0	10	10	13.465
2	20	20	15	12.081
…	…	…	…	…
18	80	20	25	14.301
19	90	30	10	50.009
…	…	…		…
29	40	10	10	16.262

To evaluate the effect of variables presented in Figure 1, 29 different experiments have been designed with the help of Hammersley sequence sampling technique so that all design space can be covered uniformly. Table 3 contains the data related to the designed computer experiments. Geometrical model of projectile for samples 7, 9, 10 and 17 are depicted in Figure 2. In all finite element models impact velocity has been considered to be 200 meters per second and all the analysis have been carried out in a symmetric plane. The three dimensional element C3D8R mesh type has been used for meshing both projectile and target. A concentrated mass of 150 kg in the end of the projectile has been considered as well. Qualitative results of modeling for the models 9 and 17 are illustrated in Figure 3.

Velocity drop is one of the objective functions which is regarded in this paper, can be stated mathematically through Equation (9).

$$\Delta v = Initial\,Velocity - Residual\,Velocity = v_i - v_r \quad (9)$$

The value of velocity drop (Δv) for the defined models is shown in Table 3.

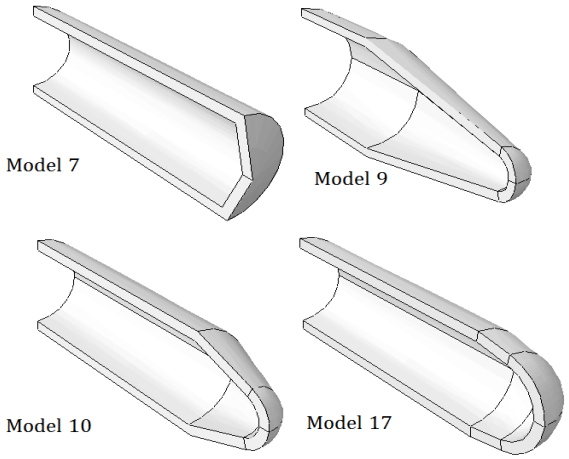

Figure 2. Three dimensional visualization of the projectile belonging to models 7, 9, 10 and 17

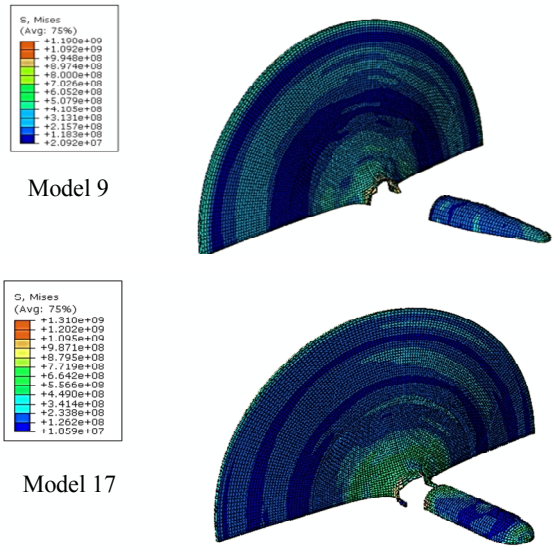

Figure 3. Visualization of finite element results for the samples 9 and 17

5. MULTI-LAYERED FEED-FORWARD NEURAL NETWORKS

In principle, neural networks have the power of a universal approximator, i.e. they can realize an arbitrary mapping of one vector space onto another vector space. The main advantage of neural networks is the fact that they have ability to use some priori unknown information hidden in data (but they are not able to extract it). Process of *capturing* the unknown information is called *learning of neural network* or *training of neural network*. In mathematical formalism *learning* means adjusting the weight coefficients in such a way that some conditions are satisfied. Multi-Layered feed-forward (MLF) neural networks, trained with a back-propagation learning algorithm, are the most popular neural networks and have been applied to a wide variety of problems [27, 28]. A MLF neural network consists of neurons that are ordered into layers. The first layer is called the input layer, the last one is called the output layer, and the layers between are hidden layers. A surrogate model using MLF neural networks is constructed from computer experiment results to estimate projectile velocity drop. This MLF model consists of two hidden layers with 4 and 2 neurons in the first and second hidden layers respectively. *Tan-sigmoid* and *purelin* transfer functions are used for hidden and output layers respectively. It should be noted that in this paper two hidden layers have been selected for the neural networks to trace accurately nonlinearity behavior of the present phenomena. Schematic of MLF neural networks is shown in Figure 4.

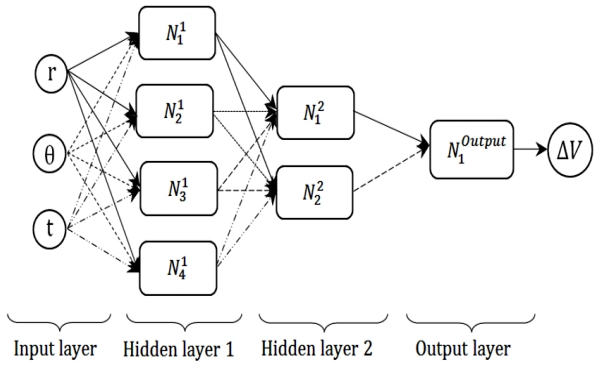

Figure 4. Schematic of MLF neural network with two hidden layers.

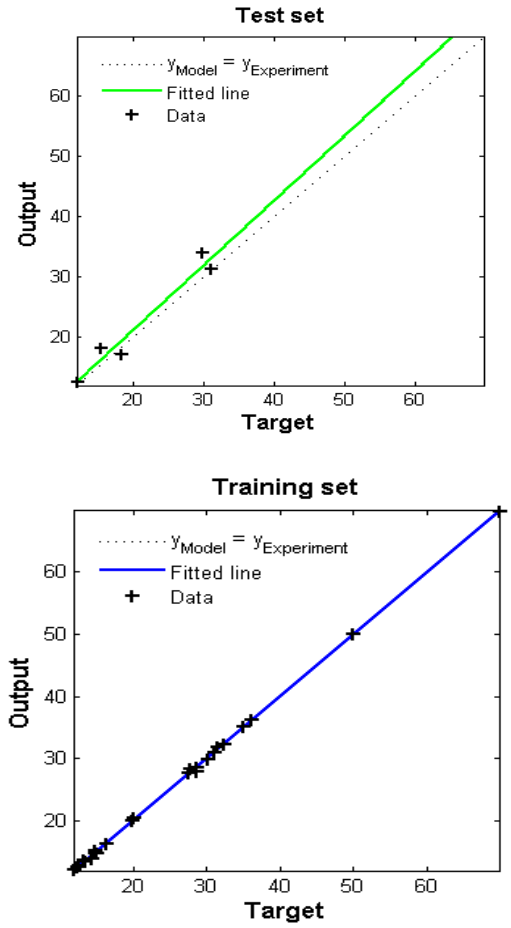

Figure 5. Representation of MLF neural networks accuracy using linear regression plot for train and test data set

TABLE 4. Statistical measures of the obtained MLF models for tracing velocity drop behavior for both train and test data

Data set	RMSE	MAPE (%)	R^2
Train set	0.0031	1.0668	0.9996
Test set	2.8446	8.5142	0.9133

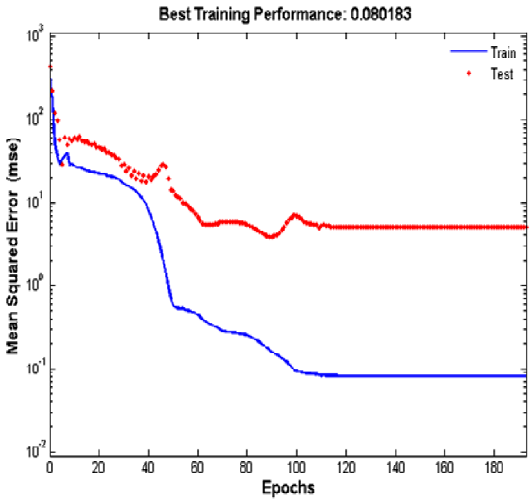

Figure 6. Error convergence history of train and test data set

A back-propagation (BP) algorithm with Levenberg-Marquardt (LM) optimization technique was employed to train MLF-type neural network. By reducing mean square error (MSE) for each epoch the accuracy of the networks was improved. To reveal the accuracy of the surrogate model (MLF neural network), Table 4 and Figure 5 are given as quantitative and qualitative representations. Figure 6 also has been committed to show convergence history of train and test data set error during the process of neural network training.

The surrogate model obtained in this section is utilized as one of the objective functions involved in Pareto multi-objective optimization process. The results of this optimization process may unveil some interesting and important optimal design principles that would not have been obtained without the use of a multi-objective optimization approach.

6. MULTI-OBJECTIVE SHAPE OPTIMIZATION OF PROJECTILE TIP

Multi-objective optimization, which is also called multi criteria optimization or vector optimization, has been defined as finding a vector of decision variables satisfying constraints to give acceptable values to all objective functions [29, 30]. In these problems, there are several objectives or cost functions (a vector of objectives) to be optimized (minimized or maximized) simultaneously. These objectives often conflict with each other so that improving one of them will deteriorate another. Therefore, there is no single optimal solution as the best with respect to all the objective functions. Instead, there is a set of optimal solutions, known as Pareto optimal solutions or Pareto front [13-15] for multi-objective optimization problems. The

concept of Pareto front or set of optimal solutions in the space of objective functions in MOPs stands for a set of solutions that are non-dominated to each other but are superior to the rest of the solutions in the search space. Each solution of the Pareto set includes at least one objective inferior to that of another solution in that Pareto set, although both are superior to others in the rest of search space. Such problems can be mathematically defined as:

Find the vector $X^* = [x_1^*, x_2^*, \dots, x_n^*]$to optimize

$$F(X) = [f_1(X), f_2(X), \dots, f_k(X)]^T \quad (10)$$

subject to m inequality constraints

$$g_i(X) \le 0 \ , \ i = 1 \ to \ m \quad (11)$$

and p equality constraints

$$h_j(X) = 0 \quad , \quad j = 1 \ to \ p \quad (12)$$

where $X^* \in \Re^n$ is the vector of decision or design variables, and $F(X) \in \Re^n$ is the vector of objective functions, which must each be either minimized or maximized. However, without loss of generality, it is assumed that all objective functions are to be minimized. Such multi-objective minimization based on Pareto approach can be conducted using some definitions.

A vector $U = [u_1, u_2, \dots, u_k] \in \Re^k$ is dominant to vector $V = [v_1, v_2, \dots, v_k] \in \Re^k$ (denoted by U$\prec V$) if and only if $\forall i = \{1, 2, \dots, k\}, \ u_i \le v_i \wedge \ \exists j \in \{1, 2, \dots, k\} : u_i < v_i$. In other words, there is at least one u_j which is smaller than v_j whilst the remaining u's are either smaller or equal to corresponding v's. A point $X^* \in \Omega$ is a feasible region in $\Re^k$ satisfying Equations (11) and (12)) is said to be Pareto optimal (minimal) with respect to all $X \in \Omega$ if and only if $F(X^*) \prec F(X)$. Alternatively, it can be readily restated as: $\forall i = \{1, 2, \dots, k\}, \ \forall X \in \Omega - \{X^*\} f_i(X^*) \le f_i(X) \wedge \ \exists j \in \{1, 2, \dots, k\} : f_j(X^*) < f_j(X)$. In other words, the solution X^* is said to be Pareto optimal (minimal) if no other solution can be found to dominate X^* using the definition of Pareto dominance. For a given MOP, a Pareto set P*is a set in the decision variable space consisting of all the Pareto optimal vectors $P^* = \{X \in \Omega | \nexists \acute{X} \in \Omega : F(\acute{X}) \prec F(X)$. In other words, there is no other $\acute{X}$ as a vector of decision variables in Ω that dominates any $X \in P^*$. For a given MOP, the Pareto front PF is a set of vector of objective functions which are obtained using the vectors of decision variables in the Pareto set P^*, that is

$$\text{PF}^* = \{F(X) = \big(f_1(X), f_2(X), \dots, f_k(X)\big) : X \in P^*\}.$$

In other words, the Pareto front PF is a set of the vectors of objective functions mapped from P^*.

Evolutionary algorithms have been widely used for multi-objective optimization because of their natural properties suited for these types of problems. This is mostly because of their parallel or population-based search approach. Therefore, most of the difficulties and deficiencies within the classical methods in solving multi-objective optimization problems are eliminated. For example, there is no need for either several runs to find the Pareto front or quantification of the importance of each objective using numerical weights. In this paper, modified NSGA-II which has been used successfully in the previous researches [16, 17] has been employed for multi- objective optimization process.

In order to investigate the optimal shape of projectile tip, three objective functions have been involved in optimization process. Velocity drop as one of the objective functions has been estimated from computer experimental results using MLF-type neural network. The two other objective functions namely, weight and inner volume of the projectile can be stated explicitly as a mathematical formulation. For evaluating inner volume as an explicit mathematical formula, it can be divided into three parts (see Figure 7) with the help of geometry and calculus, inner volume can be expressed as follows:

$$\begin{aligned}
&\acute{r} = r - t; \ \acute{R} = 100 - t, \ \acute{H} = \tfrac{\acute{R} - \acute{r}\cos\theta}{\tan\theta}, \\
&\acute{V}_1 = \ \pi\acute{R}^2\big(600 - \acute{H} - \acute{r}(1 - \sin\theta)\big), \\
&\acute{V}_2 = \tfrac{\pi}{3}\acute{H}\big(\acute{R}^2 + \acute{r}\acute{R} + \acute{r}^2\big), \\
&\acute{V}_3 = \pi\acute{r}^3\left(\tfrac{\sin^3\theta}{3} - \sin\theta + \tfrac{2}{3}\right), \\
&Inner\ Volume = \acute{V} = \acute{V}_1 + \acute{V}_2 + \acute{V}_3,
\end{aligned} \quad (13)$$

Mass can be calculated through difference between total volume and inner volume multiplied by density. Hence, the governing equation for the mass can be formulated as follows:

$$\begin{aligned}
&R = 100, \ H = \tfrac{R - r\cos\theta}{\tan\theta}, \\
&V_1 = \ 100^2\pi(600 - H - r(1 - \sin\theta)), \\
&V_2 = \tfrac{\pi}{3}H(100^2 + 100r + r^2), \\
&V_3 = \pi r^3\left(\tfrac{\sin^3\theta}{3} - \sin\theta + \tfrac{2}{3}\right), \\
&Total\ volume = V = V_1 + V_2 + V_3, \\
&Mass = M = \rho\big(V - \acute{V}\big),
\end{aligned} \quad (14)$$

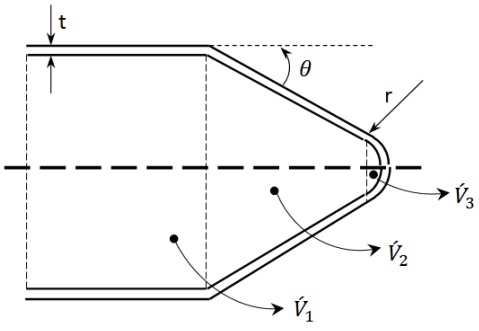

Figure 7. Inner volume of the projectile has been divided to three parts

The multi-objective shape optimization of projectile tip will allow finding trade-off optimum design points from the view point of all three objective functions simultaneously. This optimization problem can be formulated in the following form:

Design vector:[tip radius, tip angle, thickness of projectile wall]= $[r, \theta, t]$
Bounds of design variables:
$0 < r < 90;\ 10 < \theta < 80;\ 10 < t < 25$
Objective functions: (15)

$$\begin{aligned} min\ \Delta v &= f_1(r,\theta,t) \\ min\ W &= f_2(r,\theta,t) \\ max\ V &= f_3(r,\theta,t) \end{aligned}$$

A population of 100 individuals with a crossover probability of 0.8 has been used in 1000 generations for this three-objective optimization problem. Figure 8 depicts the non-dominated individuals of three-objective optimization in the plane of Δv-V. Pareto front of two-objective optimization of velocity drop and inner volume has been also depicted in this figure. Such non-dominated individuals of three-objective optimization in the plane of Δv-W and W-V together with corresponding Pareto fronts are shown in Figures 9 and 10, respectively.

As can be seen, there are some points in each plane that may dominate some other points when considering two-objective optimization results. However, these points are all non-dominated when considering all three objectives simultaneously. For multi-objective optimization problem with three objective functions a three-dimensional graph of non-dominated points can be presented which is called Pareto surface (see Figure 11).

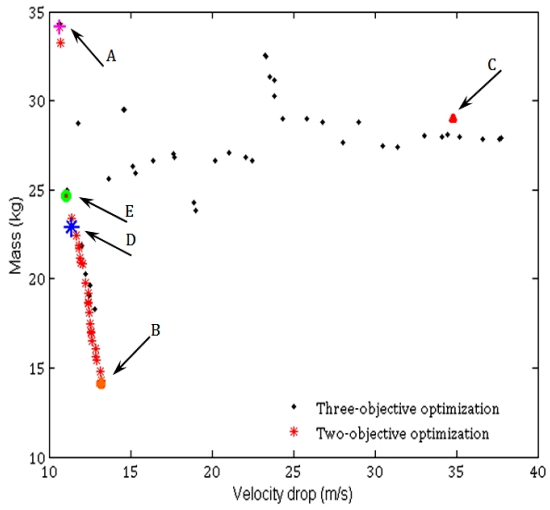

Figure 8. Pareto surface in view of Velocity drop-Mass plane to represent corresponding Pareto front and optimal desired points

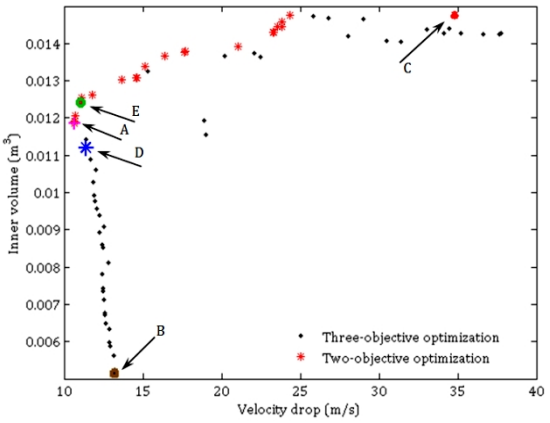

Figure 9. Pareto surface in view of Velocity drop-Mass plane to represent corresponding Pareto front and optimal desired points

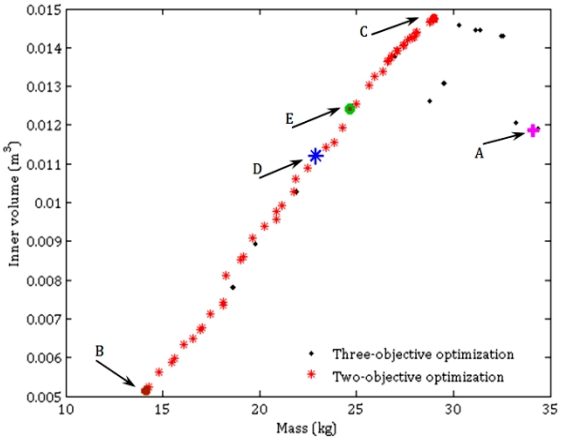

Figure 10. Pareto surface in view of Mass-Inner volume plane to represent corresponding Pareto front and optimal desired points

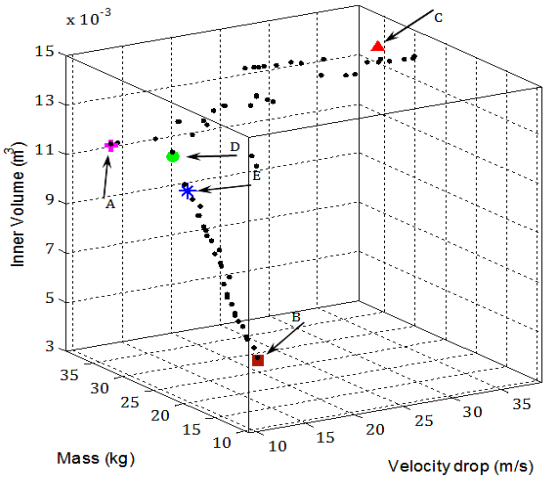

Figure 11. Pareto surface of three-objective optimization of Velocity drop-Mass-Inner volume

TABLE 5. The values of objective functions and their associated design variables of the optimum desired points

Optimum Desired Points	r (mm)	θ (degree)	t (mm)	Velocity drop (m/s)	Mass (kg)	Inner volume (m^3)
A	34.162	29.709	13.679	10.65	34.117	0.01184
B	0	10	10	13.227	14.135	0.00514
C	44.959	80	10	34.819	29.015	0.01475
D	12.96	21.144	10	11.39	22.892	0.0112
E	12.97	29.709	10	11.024	24.634	0.01241

It is now desired to find a trade-off optimum design points out of all non-dominated three-objective optimization process compromising all objective functions. This can be achieved by two different methods employed in this paper, namely nearest to ideal point method and Mapping method.

In the nearest to ideal point method, first, an ideal point with the best values of each objective functions is considered. Secondly, the distances among all non-dominated points to the ideal point are calculated. In this method, the desired point represents minimum distance to the ideal point. In the mapping method, the values of objective functions of all non-dominated point are mapped into interval 0 and 1.

Using the sum of these values for each non-dominated point, the desired point simply represents the minimum of the sum of those values.

The points *A*, *B* and *C* represent minimum velocity drop, minimum weight and maximum inner volume, respectively, which can be achieved also in single objective optimization process. In addition, by applying nearest to ideal point method and Mapping method on the results of three-objective optimization, optimum desired points D and E have been obtained. These optimum design points could be the trade-off optimum choices when considering the optimum values of three objectives. According to Figures 8 to 10, optimum design points D and E are located close to the Pareto front which demonstrates such important optimal design fact. The values of design variables and objective functions for the points A to E are represented in Table 5.

To evaluate the worthiness of an optimum design point from the view point of *ith* objective function a criterion, namely Optimum Points Worthiness (*OW*) is proposed and employed in this paper in the following form:

$$OW(p, f_i) = \frac{p_i - f_{i,B}}{f_{i,W} - f_{i,B}} \times 100 \quad (16)$$

where p and f_i are the corresponding optimum points and *ith* objective function, respectively. p_i is the value of *ith* objective function at the point p.$f_{i,B}$, and f_{iW} are also the best and worst values of the *ith* objective function in all of the obtained non-dominated optimum points. To show the efficiency of the nearest to ideal point method and Mapping method, *OW* coefficients can be obtained for the points D and E. Simply, $OW(D,f_1)$, $OW(D,f_2)$ and $OW(D,f_3)$ are equal to 2.73, 43.3 and 37.03%, respectively. Similarly, corresponding values for the optimum point E are 1.38, 51.91 and 24.4%, respectively. These values show the effectiveness of the approach of the present work. Such optimum points would not have been obtained without the use of such approach. Moreover, results of such multi-objective optimization of velocity drop, weight of projectile and inner volume provides more optional choices of design variables which can be selected from a trade-off point of view.

7. CONCLUSION

Genetic algorithm has been successfully used for multi-objective Pareto based shape optimization of a projectile tip. An efficient and accurate surrogate model to simulate velocity drop has been created using MLF-type neural networks from some numerically obtained input-output data extracted from the finite element modeling. The other two objectives, namely mass and inner volume have been formulated using explicit mathematical statements. These models then have been used in evolutionary multi-objective Pareto based optimization process. The multi-objective shape optimization of projectile tip led to the discovering some important trade-offs among those objective functions. Such combined application of MLF neural network modeling of numerical input-output data and subsequent non-dominated Pareto optimization process of the obtained meta-model is very promising in discovering useful and interesting design relationships.

8. REFERENCES

1. Marom, I. and S. Bodner, "Projectile perforation of multi-layered beams", DTIC Document, (1978)
2. Corran, R., P. Shadbolt, and C. Ruiz, "Impact loading of plates—an experimental investigation", ***International Journal of Impact Engineering,***. Vol. 1, No. 1, (1983), 3-22.

3. Nurick, G. and C. Walters. "The ballistic penetration of multiple thin plates separated by an air gap", SEM Spring Conference on Experimental Mechanics, (1990).
4. Gupta, N. and V. Madhu, "Normal and oblique impact of a kinetic energy projectile on mild steel plates", ***International Journal of Impact Engineering***, Vol. 12, No. 3, (1992), 333-343.
5. Gupta, N. and V. Madhu, "An experimental study of normal and oblique impact of hard-core projectile on single and layered plates", ***International Journal of Impact Engineering***, Vol. 19, No. 5, (1997), 395-414.
6. Børvik, T., "Perforation of 12mm thick steel plates by 20mm diameter projectiles with flat, hemispherical and conical noses: part I: experimental study", ***International Journal of Impact Engineering,*** Vol. 27, No. 1, (2002), 37-64.
7. Børvik, T., et al., "Perforation of 12mm thick steel plates by 20mm diameter projectiles with flat, hemispherical and conical noses: part II: numerical simulations", ***International Journal of Impact Engineering***, Vol. 27, No. 1, (2002), 37-64.
8. Nilakantan, G., "Finite element analysis of projectile size and shape effects on the probabilistic penetration response of high strength fabrics", ***Composite Structures***, Vol. 94, No. 5, (2012). 1846-1854.
9. Wei, Z, "Experimental investigation on the ballistic performance of monolithic and layered metal plates subjected to impact by blunt rigid projectiles", ***International Journal of Impact Engineering***, Vol. 49, (2012), 115-129.
10. Iqbal, M.A., "Experimental and numerical studies of double-nosed projectile impact on aluminum plates", ***International Journal of Impact Engineering,*** Vol. 54, (2013)**,** 232-245.
11. Deb, K., "A fast and elitist multiobjective genetic algorithm: NSGA-II", ***Evolutionary Computation, IEEE Transactions on,*** Vol. 6, No. 2, (2002), 182-197.
12. Nariman-Zadeh, N., "Inverse modelling of multi-objective thermodynamically optimized turbojet engines using GMDH-type neural networks and evolutionary algorithms", ***Engineering Optimization,*** Vol. 37, No. 5, (2005), 437-462.
13. Osyczka, A., "Multicriteria optimization for engineering design", ***Design Optimization,*** Vol. 1, (1985), 193-227.
14. Fonseca, C.M. and P.J. Fleming. "Genetic algorithms for multiobjective optimization: Formulation, discussion and generalization", in Proceedings of the fifth international conference on genetic algorithms, San Mateo, California, (1993)
15. Coello, C. A. C., G. B. Lamont, and D. A. Van Veldhuizen, "Evolutionary algorithms for solving multi-objective problems", Springer, Vol. 5. (2007):.
16. Khakhali, A., "Reliability-based robust multi-objective crashworthiness optimisation of S-shaped box beams with parametric uncertainties", ***International Journal of Crashworthiness***, Vol. 15, No. 4, (2010), 443-456.
17. Khalkhali, A. and H. Safikhani, "Pareto based multi-objective optimization of a cyclone vortex finder using CFD, GMDH type neural networks and genetic algorithms", ***Engineering Optimization***, Vol. 44, No. 1, (2012), 105-118.
18. Åström, K. and P. Eykhoff, "System identification—a survey", ***Automatica,*** Vol. 7, No. 2, (1971), 123-162.
19. Sanchez, E., T. Shibata, and L.A. Zadeh, "Genetic algorithms and fuzzy logic systems: Soft computing perspectives", ***World Scientific Publishing Company Incorporated***, Vol. 7, (1997)
20. Sacks, J., "Design and analysis of computer experiments", ***Statistical Science***, Vol. 4, No. 4, (1989), 409-423.
21. Simpson, T. W., "Metamodels for computer-based engineering design: survey and recommendations", ***Engineering With Computers***, Vol. 17, No. 2, (2001), 129-150.
22. Tang, B., "Orthogonal array-based Latin hypercubes", ***Journal of the American Statistical Association***, Vol. 88, No. 424, (1993), 1392-1397.
23. McKay, M. D., R. J. Beckman, and W. J. Conover, "Comparison of three methods for selecting values of input variables in the analysis of output from a computer code", ***Technometrics***, Vol. 21, No. 2, (1979), 239-245.
24. Kalagnanam, J. R. and U. M. Diwekar, "An efficient sampling technique for off-line quality control", ***Technometrics,*** Vol. 39, No. 3, (1997), 308-319.
25. Johnson, G.R. and W.H. Cook. "A constitutive model and data for metals subjected to large strains, high strain rates and high temperatures" in Proceedings of the 7th International Symposium on Ballistics, The Hague, Netherlands: International Ballistics Committee, (1983).
26. Jaspers, S. and J. Dautzenberg, "Material behaviour in conditions similar to metal cutting: flow stress in the primary shear zone", ***Journal of Materials Processing Technology***, Vol. 122, No. 2, (2002), 322-330.
27. Wang, G.G. and S. Shan, "Review of metamodeling techniques in support of engineering design optimization", ***Journal of Mechanical Design***, Vol. 129, No. 4, (2007), 370.
28. Cybenko, G., "Approximation by superpositions of a sigmoidal function", ***Mathematics of Control, Signals, and Systems (MCSS)***, Vol. 2, No. 4, (1989), 303-314.
29. Hornik, K., M. Stinchcombe, and H. White, "Multilayer feedforward networks are universal approximators", ***Neural Networks***, Vol. 2, No. 5, (1989), 359-366.
30. Coello, C. and A.D. Christiansen, "Multiobjective optimization of trusses using genetic algorithms", ***Computers & Structures***, Vol. 75, No. 6, (2000), 647-660.

Multi-objective Optimization of a Projectile Tip for Normal Penetration

A. Khalkhali[a], S. Roshanfekr[b]

[a] *School of Automotive Engineering, Iran University of Science and Technology, Tehran, Iran*
[b] *School of Mechanical Engineering, Islamic Azad University, Takestan branch, Qazvin, Iran*

P A P E R I N F O

Paper history:
Received 30 January 2013
Received in revised form 04 March 2013
Accepted 18 April 2013

Keywords:
Projectile
Impact
Finite Element Method
Neural Networks
Multi-objective Optimization
NSGA-II

چکیده

هدف اصلی در این مقاله بهینه سازی شکل نوک یک پرتابه در برخورد و نفوذ قائم با در نظر گرفتن افت سرعت، وزن و حجم داخلی پرتابه به عنوان سه تابع هدف متضاد است. برای این منظور، ابتدا با استفاده از نرم فزار ABAQUS/Explicit مدل‌سازی اجزای محدود انجام و با نظر گرفتن ابعاد هندسی مختلف، نفوذ پرتابه بررسی شد. آزمایش‌های کامپیوتری با استفاده از دنباله‌ی همرسلی طرحی شد. در قدم بعدی از مجموعه‌ی نتایج مدل‌سازی اجزای محدود، به عنوان داده‌های خام برای آموزش و آزمایش شبکه‌های عصبی فیدفوروارد به منظور دست‌یابی به یک مدل ریاضی برای بیان افت سرعت استفاده شد. برای وزن و حجم پرتابه نیز روابط صریح ریاضی توسعه داده شد. از روابط به دست آمده برای بهینه‌سازی چندهدفی با استفاده از الگوریتم ژنتیک استفاده شد. نتایج به دست آمده روابط سودمندی را در طراحی بهینه نمایش می‌دهد که تنها با به کارگیری بهینه‌سازی چندهدفی مدل ریاضی استخراج شده از نتایج حل اجزای محدود قابل تحصیل است.

doi: *10.5829/idosi.ije.2013.26.10a.12*